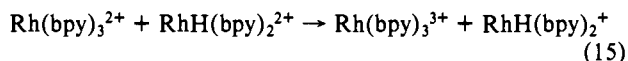
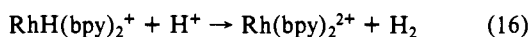


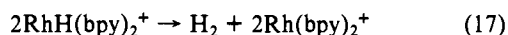
nor Rh(II), is capable of generating H<sub>2</sub> by itself at appreciable rates in the uncatalyzed systems. Nevertheless, of all these intermediates, the most logical candidate<sup>4</sup> for uncatalyzed H<sub>2</sub> formation is RhH(bpy)<sub>2</sub><sup>2+</sup>. Now, during the continuous radiolysis and photolysis experiments in the natural pH region, Rh(bpy)<sub>3</sub><sup>3+</sup>, which is a good reductant, could be capable of reducing RhH(bpy)<sub>2</sub><sup>2+</sup> (reaction 15). Kirch et al.<sup>4</sup> report that the third step



in the reduction of Rh(bpy)<sub>3</sub><sup>3+</sup> occurs at -1.15 V at pH 10.7 and -0.90 V at pH 7.0. From what we now know about the various forms of Rh(bpy)<sub>2</sub><sup>2+</sup>, it follows that RhH(bpy)<sub>2</sub><sup>2+</sup> is a stronger oxidant than is Rh(bpy)<sub>2</sub>(OH)<sub>n</sub><sup>1-n</sup>. Interaction of RhH(bpy)<sub>2</sub><sup>2+</sup> with H<sup>+</sup> could lead to H<sub>2</sub> according to reaction 16. Another



possible pathway, represented by reaction 17, is similar to the



binuclear homolytic mechanism for the generation of H<sub>2</sub> from hydridocobaloxime.<sup>33</sup> According to this kinetic scheme, the yield of H<sub>2</sub> should increase to a plateau as RhH(bpy)<sub>2</sub><sup>2+</sup> builds up in the system and reaches a steady-state concentration.<sup>34</sup> Our

(33) Chao, T.-H.; Espenson, J. H. *J. Am. Chem. Soc.* 1978, 100, 129.

determination of the dependence of G(H<sub>2</sub>) as a function of irradiation time is in accord with this mechanism. Experiments designed to optimize the uncatalyzed yield of H<sub>2</sub> are currently in progress.

### Conclusions

It is clear that the one-electron reduction of Rh(bpy)<sub>3</sub><sup>3+</sup> in aqueous solution yields a very rich chemistry that must be understood in detail if complex redox systems involving this substance are to be utilized. Both Rh(bpy)<sub>3</sub><sup>2+</sup> and Rh(bpy)<sub>2</sub><sup>2+</sup> are involved in highly complex interlocking ligand-labilization, acid-base, redox, and aggregation reactions. Using the symbol Rh-L to represent tris(bpy)species, Rh-L/2 to represent a species with a monodentate ligand, and Rh to represent ligand-labilized species which may or may not contain coordinated H<sub>2</sub>O or OH<sup>-</sup>, we summarize our current findings in Scheme I.

**Acknowledgment.** The authors thank Professor V. Balzani for his interest in this work and helpful discussions. Assistance by the Linac staff (Dr. A. Martelli, Dr. G. Roffi, E. Gardini, G. Mancini, and V. Raffaelli), skillful glassblowing by L. Minghetti, and the drawing of the figures by L. Ventura is gratefully acknowledged. They also thank Dr. C. Cruetz for providing to them a preprint of ref 5 prior to publication.

(34) As the concentration of RhH(bpy)<sub>2</sub><sup>2+</sup> builds up, direct reduction of that species to RhH(bpy)<sub>2</sub><sup>+</sup> by radiation-generated reducing radicals or, in the case of the photochemical system, \*Ru(bpy)<sub>3</sub><sup>2+</sup> can occur.

## The Nonadiabaticity Problem of Outer-Sphere Electron-Transfer Reactions. Reduction and Oxidation of Europium Ions

V. Balzani,<sup>\*1a,b</sup> F. Scandola,<sup>1c</sup> G. Orlandi,<sup>1a,b</sup> N. Sabbatini,<sup>1b</sup> and M. T. Indelli<sup>1c</sup>

*Contribution from the Istituto di Fotochimica e Radiazioni d'Alta Energia del C.N.R., Bologna, Istituto Chimico "G. Ciamician" dell'Università, Bologna, and Centro di Studio sulla Fotochimica e Reattività degli Stati Eccitati dei Composti di Coordinazione del C.N.R., Università di Ferrara, Italy. Received May 16, 1980*

**Abstract:** A new type of approach to the nonadiabaticity problem of outer-sphere electron-transfer reactions is presented. The approach is based on the analysis of the change in the rate constants of the reactions of the species under consideration with a homogeneous family of redox partners having variable redox potential. In favorable cases such an analysis allows us to disentangle the effects of intrinsic barrier (nuclear term) and nonadiabaticity (electronic term) on the rate constant. The literature data for the reactions of Ru(NH<sub>3</sub>)<sub>6</sub><sup>2+</sup>, Ru(NH<sub>3</sub>)<sub>6</sub><sup>3+</sup>, Fe<sup>2+</sup>, Fe<sup>3+</sup>, Eu<sup>2+</sup>, and Eu<sup>3+</sup> with a homogeneous family of partners have been collected and the log *k*<sub>12</sub> vs. Δ*G* plots have been drawn and examined. For Ru(NH<sub>3</sub>)<sub>6</sub><sup>2+</sup> and Fe<sup>2+</sup> the plots indicate small (Ru(NH<sub>3</sub>)<sub>6</sub><sup>2+</sup>) and large (Fe<sup>2+</sup>) intrinsic barriers and adiabatic or nearly adiabatic behavior (adiabaticity factor, κ > 10<sup>-3</sup>) in the Δ*G* range 0 to -1.5 eV. For Eu<sup>2+</sup>, different plots are obtained for Eu<sup>2+</sup> oxidation or Eu<sup>3+</sup> reduction. These plots suggest a strongly nonadiabatic behavior of europium ions (κ ≈ 10<sup>-6</sup>) at moderately negative Δ*G* values. A theoretical estimate of the adiabaticity factor based on spectroscopic information yields κ ≤ 10<sup>-5</sup> for electron-transfer reactions between ground-state Eu<sup>2+</sup> ions and adiabatic-type partners. At large and negative Δ*G* values more efficient but different channels become available for Eu<sup>2+</sup> oxidation or Eu<sup>3+</sup> reduction. These channels are tentatively assigned to paths involving different charge-transfer intermediates. The role played by excited states in electron-transfer reactions is discussed.

The rate constants of outer-sphere electron-transfer reactions (eq 1) are usually discussed in the literature on the basis of the



Marcus equation (eq 2),<sup>2</sup> where *Z* is the collision frequency of

$$k_{12} = pZ e^{-(\Delta G^\ddagger + w_r)/RT} \quad (2)$$

neutral molecules in solution, Δ*G*<sup>‡</sup> is the free activation energy, *w*<sub>r</sub> is the work required to bring the reactants together, and *p* is the probability of electron transfer in the activated complex. According to Sutin,<sup>3-5</sup> eq 2 can be recast as in eq 3, where *K*<sub>0</sub> is

(1) (a) Istituto di Fotochimica e Radiazioni d'Alta Energia del C.N.R. (b) Istituto Chimico "G. Ciamician" dell'Università. (c) Centro di Studio sulla Fotochimica e Reattività degli Stati Eccitati dei Composti di Coordinazione del C.N.R.

(2) Marcus, R. A. *Faraday Discuss. Chem. Soc.* 1960, 29, 21; *Annu. Rev. Phys. Chem.* 1964, 15, 155; *J. Chem. Phys.* 1965, 43, 679; *Electrochim. Acta* 1968, 13, 995. In "Tunneling in Biological Systems"; Chance, B., De Vault, D. C., Frauenfelder, H., Marcus, R. A., Schrieffer, J. R., Sutin, N., Eds.; Academic Press: New York, 1979; p 109.

$$k_{12} = K_0 k_e = K_0 \kappa \frac{kT}{h} e^{-\Delta G^*/RT} \quad (3)$$

the equilibrium constant for the formation of the precursor complex,  $k_e$  is the unimolecular rate constant for the reaction of the precursor complex,  $\kappa$  is the probability of electron transfer in the activated complex,  $kT/h$  is the universal frequency of the absolute reaction rate theory, and  $\Delta G^*$  is the free activation energy. These classical equations, like the quantum mechanical equation in the high-temperature limit,<sup>6</sup> express the rate constant as a product of an electronic term associated to  $p$  or  $\kappa$  and a nuclear term ( $e^{-\Delta G^*/RT}$ ).

The electronic term is closely related to the strength of the electronic interaction between the reactants,  $V$  (in quantum mechanical language, this is the coupling between the initial and final electronic states of the supermolecule  $A_1A_2$ ).<sup>7</sup> When such an interaction is strong enough ( $\geq 100 \text{ cm}^{-1}$ ), the probability of electron transfer is unity and thus  $k_{12}$  is essentially independent of  $V$ . In such a case, the reaction is said to be *adiabatic*. When the electronic interaction is weak, both the semiclassical Landau-Zener theory<sup>8</sup> and the quantum mechanical treatments<sup>7,9</sup> show that the probability of electron transfer is proportional to the square of the interaction  $V$  and is lower than unity. In this case the reaction is called *nonadiabatic*.

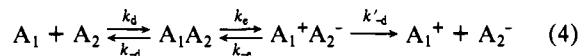
In the quantum mechanical approach the nuclear term  $e^{-\Delta G^*/RT}$  represents the Franck-Condon factor for low-energy vibrations ( $\hbar\omega \ll kT$ ) such as the solvent modes which are "reorganized" by the electron transfer. In the classical approach  $\Delta G^*$  is expressed as a function of the so-called intrinsic barrier  $\Delta G^*(0)$  and of the free energy change  $\Delta G$  (see below).

In discussing the experimental results of outer-sphere electron-transfer processes, it has been common practice to neglect the electronic term by assuming that  $p$  (or  $\kappa$ ) is equal to unity (adiabaticity assumption). Attention has usually been focussed on the nuclear term, and the differences among the rate constants of exchange reactions, whose values range from immeasurably small to almost diffusion controlled, have generally been ascribed to differences in the intrinsic barriers.<sup>3,10</sup> Suggestions or indications of nonadiabatic behavior have been recently discussed for some specific reactions,<sup>3,4,11-16</sup> and Sutin<sup>3,15</sup> has also put forward a nonadiabatic version of the Marcus cross relation; however there is still a general feeling that nonadiabaticity does not play an important role in outer-sphere electron-transfer processes of coordination compounds.<sup>3,4,10,11,15</sup>

Taube<sup>11-13</sup> has recently discussed several different approaches to the nonadiabaticity problem. In this paper we propose another type of approach which descends from our photochemical experience and we apply this approach to the electron-transfer reactions of Eu(II) and Eu(III) ions. A more detailed discussion of the nonadiabaticity problem and a critical reexamination of a larger number of literature data will be given in subsequent papers.

### Approach to the Nonadiabaticity Problem. Relationship between Rate Constants and Free Energy Change

Reaction 1 can be considered to occur according to the sequence of elementary steps given in eq 4,<sup>17-20</sup> where  $k_d$  is the diffusion



rate constant,  $k_{-d}$  and  $k'_{-d}$  are the rate constant for dissociation of the precursor and successor complex, and  $k_e$  and  $k_{-e}$  are unimolecular rate constants for electron transfer. The experimental rate constant of eq 1 can be expressed as a function of the rate constants of eq 4 by using steady-state methods.

$$k_{12} = \frac{k_d}{1 + \frac{k_{-d}}{k_e} \left(1 + \frac{k_{-e}}{k'_{-d}}\right)} = \frac{k_d}{1 + \frac{k_{-d}}{k_e} + \frac{k_{-d}k_{-e}}{k'_{-d}k_e}} \quad (5)$$

For slow electron-transfer reactions, i.e., when  $k_{-e} \ll k'_{-d}$  and  $k_e \ll k_{-d}$ , eq 5 reduces to the Sutin preequilibrium formulation (eq 3).<sup>3-5</sup> With use of a classical approach, the ratio  $k_{-e}/k_e$  is equal to  $\exp(\Delta G/RT)$  where  $\Delta G$  is the free energy change of the electron-transfer step and the rate constant of the electron-transfer step is given by eq 6, where  $k_e^0$  is the frequency factor and  $\kappa$ ,  $kT/h$ ,

$$k_e = k_e^0 e^{-\Delta G^*/RT} = \kappa \frac{kT}{h} e^{-\Delta G^*/RT} \quad (6)$$

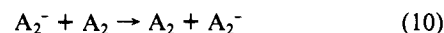
and  $\Delta G^*$  have the same meaning as above. Equation 5 can thus be written as eq 7. As first suggested by Marcus,<sup>2</sup> the free

$$k_{12} = \frac{k_d}{1 + \frac{k_{-d}}{k_e^0 e^{\Delta G^*/RT}} + \frac{k_{-d}}{k'_{-d}} e^{\Delta G/RT}} \quad (7)$$

activation energy can be expressed as a function of the free energy change and of the so-called intrinsic barrier,  $\Delta G^*(0)$ , a parameter related to the amount of distortion of both the inner coordination spheres and the outer solvation shells accompanying the electron transfer.  $\Delta G^*(0)$  can be expressed as

$$\Delta G^*(0) = \frac{\Delta G^*_{11} + \Delta G^*_{22}}{2} \quad (8)$$

where  $\Delta G^*_{11}$  and  $\Delta G^*_{22}$  are the intrinsic barriers of the exchange reactions.



The original Marcus quadratic free energy relationship<sup>2</sup> does not account for the experimental results in the exoergonic region.<sup>21</sup> As discussed elsewhere,<sup>21</sup> there are two practically equivalent empirical relationships which satisfactorily account for the experimental results and also simulate fairly well the expectations of a full quantum mechanical approach.<sup>7,9,23</sup> Equation 11 is one

$$\Delta G^* = \Delta G + \frac{\Delta G^*(0)}{\ln 2} \ln \left[ 1 + \exp \left( -\frac{\Delta G \ln 2}{\Delta G^*(0)} \right) \right] \quad (11)$$

of such *empirical* relationships.<sup>22</sup> Incorporation of eq 11 in eq 7 predicts that for a homogeneous series of electron-transfer reactions (i.e., when  $k_{en}^0$ ,  $\Delta G^*(0)$ ,  $k_d$ ,  $k_{-d}$ , and  $k'_{-d}$  are constant), a plot of  $\log k_{12}$  vs.  $\Delta G$  consists of (Figure 1) the following: (i) a plateau region for sufficiently exoergonic reactions, (ii) an

(17) Rehm, D.; Weller, A. *Isr. J. Chem.* **1970**, *8*, 259.

(18) Balzani, V.; Bolletta, F.; Gandolfi, M. T.; Maestri, M. *Top. Curr. Chem.* **1978**, *75*, 1.

(19) Indelli, M. T.; Scandola, F. *J. Am. Chem. Soc.* **1978**, *100*, 7733.

(20) Balzani, V.; Bolletta, F.; Scandola, F. *J. Am. Chem. Soc.* **1980**, *102*, 2152.

(21) Balzani, V.; Bolletta, F., *Ibid.* **1978**, *100*, 7404.

(22) Scandola, F.; Balzani, V. *J. Am. Chem. Soc.* **1979**, *101*, 6140.

(23) As previously noted,<sup>21</sup> eq 11 was first derived by Marcus (*J. Phys. Chem.* **1968**, *72*, 891) for atom- and proton-transfer reactions on the basis of the BEBO model and then used by Agmon and Levine (*Chem. Phys. Lett.* **1977**, *52*, 197) to discuss concerted reaction kinetics. We emphasize that we use eq 11 in a purely empirical way regardless of its theoretical derivation.

(24) Orlandi, G.; Monti, S.; Barigelletti, F.; Balzani, V. *Chem. Phys.* **1980**, *52*, 313.

(3) Sutin, N. *Inorg. Biochem.* **1973**, *611*.

(4) Sutin, N. In "Tunneling in Biological Systems"; Chance, B., De Vault, D. C., Frauenfelder, H., Marcus, R. A., Schrieffer, J. R., Sutin, N., Eds.; Academic Press: New York, 1979, p 201.

(5) Brown, G. M.; Sutin, N. *J. Am. Chem. Soc.* **1979**, *101*, 883.

(6) Levich, V. G. *Adv. Electrochem. Electrochem. Eng.* **1966**, *4*, 249. Dogonadze, R. R. In "Reaction of Molecules at Electrodes"; Hush, N. S., Ed.; Wiley-Interscience: London 1971; p 135.

(7) Kestner, N. R.; Logan, J.; Jortner, J. *J. Phys. Chem.* **1974**, *78*, 2148.

(8) Landau, L. D. *Phys. Z. Sowjetunion* **1932**, *2*, 46.

(9) Bixon, M.; Efrima, S. *Chem. Phys. Lett.* **1974**, *25*, 34. Ulstrup, J.; Jortner, J. *J. Chem. Phys.* **1975**, *63*, 4358. Van Duyne, R. P.; Fischer, S. F. *Chem. Phys.* **1974**, *5*, 183.

(10) For reviews, see: Bennet, L. E. *Prog. Inorg. Chem.* **1973**, *18*, 1. Pennington, D. E. *Adv. Chem. Ser.* **1978**, *No. 174*, 466.

(11) Taube, H. *Adv. Chem. Ser.* **1977**, *No. 162*, 127.

(12) Taube, H. In "Tunneling in Biological Systems"; Chance, B., De Vault, D. C., Frauenfelder, H., Marcus, R. A., Schrieffer, J. R., Sutin, N., Eds.; Academic Press: New York, 1979; p 173.

(13) Brown, G. M.; Krentzien, H. J.; Abe, M.; Taube, H. *Inorg. Chem.*, **1979**, *18*, 3374.

(14) Chan, M. S.; Wahl, A. C. *J. Phys. Chem.* **1978**, *82*, 2542.

(15) Chou, M.; Creutz, C.; Sutin, N. *J. Am. Chem. Soc.* **1977**, *99*, 5615.

(16) Buhks, E.; Bixon, M.; Jortner, J.; Navon, G. *Inorg. Chem.* **1979**, *18*, 2014.

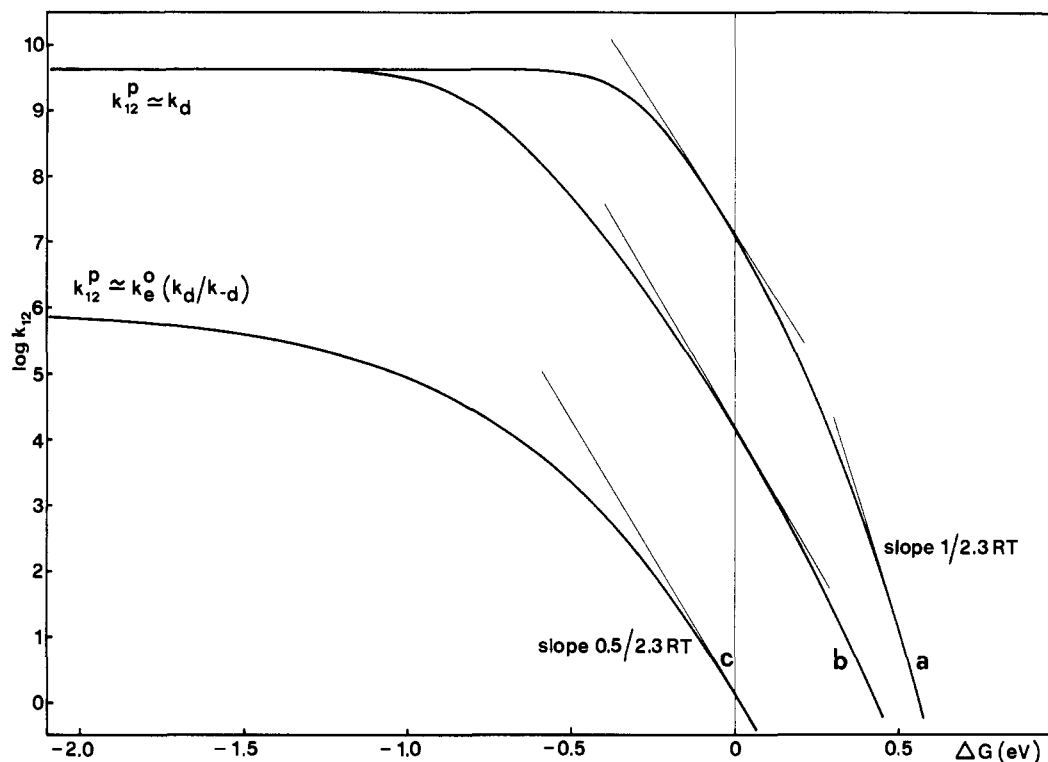


**Figure 1.** Calculated  $\log k_{12}$  vs.  $\Delta G$  plots for different intrinsic barriers and adiabaticity factors by using eq 7 and 11: (a)  $\Delta G^*(0) = 8$  kcal/mol,  $\kappa = 1$ ; (b)  $\Delta G^*(0) = 12$  kcal/mol,  $\kappa = 1$ ; (c)  $\Delta G^*(0) = 8$  kcal/mol,  $\kappa = 1 \times 10^{-7}$ . In all cases, the other parameters used were as follows:  $k_d = 4.5 \times 10^9 \text{ M}^{-1} \text{ s}^{-1}$ ;  $k_{-d} = 2.8 \times 10^9 \text{ s}^{-1}$ ;  $k'_{-d} = 2.6 \times 10^9 \text{ s}^{-1}$ ;  $T = 298 \text{ K}$ .

Arrhenius-type linear region (slope  $1/(2.3RT)$ ) for sufficiently endoergonic reactions, and (iii) a more or less wide (depending on  $\Delta G^*(0)$ ) intermediate region in which  $\log k_{12}$  increases in a complex but monotonous way as  $\Delta G$  decreases. The intermediate region is centered at  $\Delta G = 0$  where the slope of the curve is  $0.5 [1/(2.3RT)]$ .<sup>24</sup> The plateau value of  $k_{12}$ ,  $k_{12}^p$ , is given by eq 12

$$k_{12}^p = \frac{k_d k_e^0}{k_e^0 + k_{-d}} \quad (12)$$

and is equal to  $k_d$  or  $k_e^0(k_d/k_{-d})$  depending on whether  $k_e^0$  is much larger or much smaller than  $k_{-d}$ . It follows that a very low value of the frequency factor (i.e.,  $\kappa < k_{-d} h/kT$ ) is reflected in a lower than diffusion value of  $k_{12}^p$ . Thus, although a lower than diffusion plateau may also be obtained in particular cases for other reasons,<sup>24</sup> in most cases a low  $k_{12}^p$  is indicative of a nonadiabatic behavior. On the other hand, the value of the intrinsic barrier  $\Delta G^*(0)$  does not affect  $k_{12}^p$  but strongly influences the values of the rate constant in the intermediate nonlinear region. This type of approach, which in favorable cases allows to disentangle the effects of nonadiabaticity and intrinsic barrier on the rate constant, has been successfully applied to interpret the results of electron-transfer quenching of excited states.<sup>18,21</sup> More recently, it has also been extended to exchange energy-transfer processes<sup>20,26,27</sup> which are conceptually related to electron transfer.<sup>28</sup> Interestingly, in some energy-transfer cases a stepwise behavior of the  $\log k_{12}$  vs.  $\Delta G$  plots has been observed,<sup>29</sup> as expected when the process is strongly

nonadiabatic in the isoergonic region and more adiabatic reaction channels become available with increasing driving force.<sup>20</sup>

#### Electron-Transfer Reactions of Europium Ions

As mentioned in the introduction, most workers studying outer-sphere electron-transfer processes have assumed an adiabatic behavior. However, the very low self-exchange rate ( $k \leq 3 \times 10^{-5} \text{ M}^{-1} \text{ s}^{-1}$ ) of the  $\text{Eu}^{3+/2+}$  couple<sup>30</sup> has since long arisen a suspicion of nonadiabaticity. Taube<sup>31</sup> pointed out that a nonadiabatic behavior would in fact be expected for this reaction since the 4f orbitals involved in the electron transfer are strongly shielded by the 5s and 5p orbitals. He has also noted<sup>11</sup> that owing to the larger size of the europium ions, both the inner-sphere and the solvent reorganization energies must be less than for the  $\text{Fe}^{3+/2+}$  couple, whose self-exchange reaction, however, is much faster ( $k = 4 \text{ M}^{-1} \text{ s}^{-1}$ ). A number of anomalies in the kinetic behavior of ions involving f orbitals have also been considered by Taube<sup>11</sup> as suggestive of a nonadiabatic behavior. However, he seems to conclude that a definitive proof of nonadiabatic behavior of these ions is still lacking. Chou et al.<sup>15</sup> have also discussed in detail the behavior of  $\text{Eu}^{2+}$  in electron-transfer reactions and considered the possibility that nonadiabaticity, together with the failure of other assumptions of the Marcus model, may be an explanation of the observed behavior. Creutz<sup>32</sup> noted an incorrect free energy dependence of the rate constants of the  $\text{Eu}^{2+}$  and  $\text{Eu}^{3+}$  reactions with (polypyridine)ruthenium(II) complexes and concluded that there was no obvious explanation for such a behavior. In an attempt to establish whether nonadiabaticity plays an important role in the reactions of europium ions, we have applied the approach described in the previous section to some literature data concerning such reactions and we have also tried to estimate the  $\kappa$  adiabaticity factor from spectroscopic information.

**Application of the Free Energy Relationship Approach.** Theoretical expectations as well as experimental evidences indicate that the  $\text{M}(\text{LL})_3^{n+}$  complexes ( $\text{M} = \text{Cr}, \text{Fe}, \text{Ru}, \text{Os}$ ;  $\text{LL} =$

(24) Preequilibrium changes on one of the reactants may cause rate saturation below the diffusion limit.<sup>25</sup> Other factors which may probably decrease the preexponential term<sup>4,5</sup> (i.e., orientational factors and use of other nuclear frequencies in the place of the classical  $kT/h$ ) are not likely to cause  $k_{e1}^0 < k_{-d}$ .

(25) Marcus, R. A.; Sutin, N. *Inorg. Chem.* **1975**, *14*, 213.

(26) Balzani, V.; Bolletta, F.; Scandola, F.; Ballardini, R. *Pure Appl. Chem.* **1979**, *51*, 299.

(27) Balzani, V.; Indelli, M. T.; Maestri, M.; Sandrini, D.; Scandola, F. *J. Phys. Chem.* **1980**, *84*, 852.

(28) Electron-transfer processes and exchange energy-transfer processes can also be treated quantum mechanically by using the same formalism.<sup>7,23</sup>

(29) Wilkinson, F.; Farmilo, A. *J. Chem. Soc. Faraday Trans. 2* **1976**, *72*, 604.

(30) Meyer, D. J.; Garner, C. S. *J. Phys. Chem.* **1952**, *56*, 853.

(31) Taube, H. *Adv. Inorg. Chem. Radiochem.* **1959**, *1*, 47.

(32) Creutz, C. *Inorg. Chem.* **1978**, *17*, 1046.

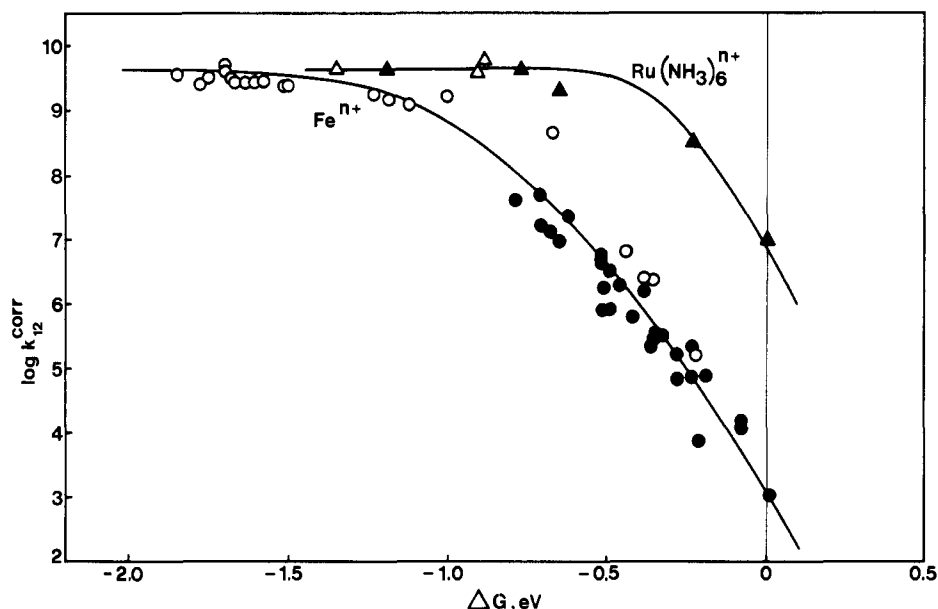


Figure 2.  $\log k_{12}^{\text{corr}}$  vs.  $\Delta G$  plots for the electron-transfer reactions involving  $\text{Ru}(\text{NH}_3)_6^{2+}$  ( $\blacktriangle$ ),  $\text{Ru}(\text{NH}_3)_6^{3+}$  ( $\triangle$ ),  $\text{Fe}^{2+}$  ( $\bullet$ ), and  $\text{Fe}^{3+}$  ( $\circ$ ). The curves represent fits on the basis of eq 7 and 11 by using the parameters given in the text.

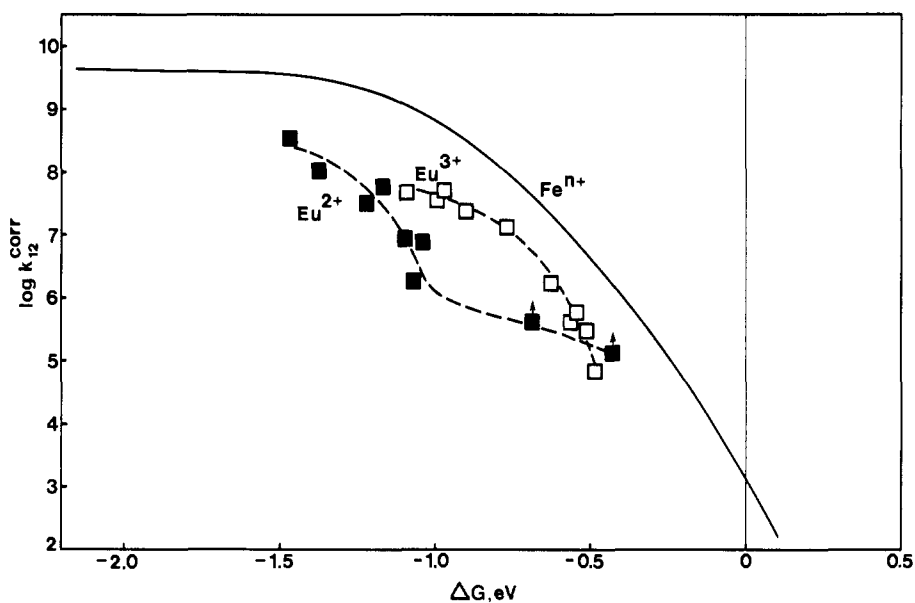


Figure 3.  $\log k_{12}^{\text{corr}}$  vs.  $\Delta G$  plots for the electron-transfer reactions involving  $\text{Eu}^{2+}$  ( $\blacksquare$ ) and  $\text{Eu}^{3+}$  ( $\square$ ). The dashed curves have only been drawn with the aim of connecting the points within the  $\text{Eu}^{2+}$  and  $\text{Eu}^{3+}$  series of reactions. The small arrows indicate that the corresponding points are lower limiting values (see text). The full curve is that for  $\text{Fe}^{n+}$  reactions shown in Figure 2.

2,2'-bipyridine (bpy) or 1,10-phenanthroline (phen) or their derivatives;  $n = 1, 2$ , or 3) in their ground or lowest excited state have small intrinsic barriers and  $\kappa$  approaching unity.<sup>4,11,12,15,33-35</sup> The complexes  $\text{Ru}(\text{NH}_3)_4(\text{bpy})^{n+}$  and  $\text{Ru}(\text{NH}_3)_5\text{X}^{n+}$  ( $\text{X} = \text{pyridine (py)}$ , nicotamide (nic), or isonicotamide (isn);  $n = 2$  or 3) are also considered to behave adiabatically and to have relatively small (and known) intrinsic barriers.<sup>5,13,15</sup> Thus, once their different intrinsic barriers are accounted for (see Appendix I), all the above complexes constitute a homogeneous family of redox reactants which allow us to explore the behavior of a species in a fairly wide  $\Delta G$  range.

The literature data,  $k_{12}^{\text{obsd}}$ , for the redox reactions between members of the above-mentioned homogeneous family and  $\text{Eu}^{2+}$ ,

$\text{Eu}^{3+}$ ,  $\text{Fe}^{2+}$ ,  $\text{Fe}^{3+}$ ,  $\text{Ru}(\text{NH}_3)_6^{2+}$ , and  $\text{Ru}(\text{NH}_3)_6^{3+}$  are collected in Table I. For the reactions involving the europium ions, the ionic strength is controlled by  $\text{Cl}^-$  ions in all but one case. Since the ionic size, the charge product, and the ionic strength are not constant (though not very different), all the observed rate constants have been made homogeneous ( $2+, 2+$  reactants,  $r = 11 \text{ \AA}$ ,  $\mu = 0.5 \text{ M}$ ) using conventional equations (see Appendix II). In addition, the rate constants of the reactions involving  $\text{Ru}(\text{NH}_3)_4\text{bpy}^{n+}$ ,  $\text{Ru}(\text{NH}_3)_5\text{X}^{n+}$ , and  $\text{Ru}(\text{NH}_3)_6^{n+}$  as redox partners have been corrected for the higher intrinsic barriers of these reactants (see Appendix I) except for the reactions involving  $\text{Eu}^{2+}$ . In the last case, in fact, the procedure outlined in Appendix I cannot be applied for lack of information on the adiabaticity coefficient of europium. It should be noted, however, that such a correction would have caused an increase in the rate constant, regardless of the actual  $\kappa$  value of  $\text{Eu}^{2+}$ . The homogenized values obtained after correction,  $k_{12}^{\text{corr}}$ , are also shown in Table I.

The values of  $\log k_{12}^{\text{corr}}$  have been plotted against  $\Delta G$  in Figures 2 and 3. As one can see, the behavior of  $\text{Fe}^{n+}$ ,  $\text{Ru}(\text{NH}_3)_6^{n+}$ , and  $\text{Eu}^{n+}$  is very different.

(33) Sutin, N. *J. Photochem.* 1979, 10, 19.

(34) Sutin, N.; Creutz, C. *Adv. Chem. Ser.* 1978, No. 168, 1.

(35) Creutz, C.; Chou, M.; Netzel, T. L.; Okumura, M.; Sutin, N. *J. Am. Chem. Soc.* 1980, 102, 1309. These authors show that the excited iron-pyridine complexes have high intrinsic barriers; reactions of such species are not considered in this paper.

Table I. Redox Reactions of  $\text{Eu}^{2+}$ ,  $\text{Fe}^{2+}$ , and  $\text{Ru}(\text{NH}_3)_6^{2+}$ 

$A_1$	redox partner, $A_2$	$k_{12}^{\text{obsd } a}$	$\mu, M$ (anion)	ref	$\Delta G,^b \text{ eV}$	$k_{12}^{\text{corr } c}$	
$\text{Eu}^{2+}$	$\text{Ru}(\text{NH}_3)_6^{3+}$	$1.5 \times 10^4$	1.0 ( $\text{Cl}^-$ )	<i>d</i>	-0.43	$1.2 \times 10^5$	
	$\text{Ru}(\text{NH}_3)_5\text{py}^{3+}$	$5.4 \times 10^4$	1.0 ( $\text{ClO}_4^-$ )	15	-0.69	$4.4 \times 10^5$	
	$^*\text{Ru}(4,7\text{-}(\text{CH}_3)_2\text{phen})_3^{2+}$	$0.70 \times 10^7$	0.5 ( $\text{Cl}^-$ )	32	-1.05	$0.70 \times 10^7$	
	$^*\text{Ru}(4,4'\text{-}(\text{CH}_3)_2\text{bpy})_3^{2+}$	$0.15 \times 10^7$	0.5 ( $\text{Cl}^-$ )	32	-1.07	$0.15 \times 10^7$	
	$^*\text{Os}(5\text{-Clphen})_3^{2+}$	$7.9 \times 10^6$	0.5 ( $\text{Cl}^-$ )	35	-1.10	$7.9 \times 10^6$	
	$^*\text{Ru}(\text{phen})_3^{2+}$	$4.9 \times 10^7$	0.5 ( $\text{Cl}^-$ )	32	-1.17	$4.9 \times 10^7$	
	$^*\text{Ru}(\text{bpy})_3^{2+}$	$2.8 \times 10^7$	0.5 ( $\text{Cl}^-$ )	32	-1.22	$2.8 \times 10^7$	
	$^*\text{Ru}(5\text{-Clphen})_3^{2+}$	$10 \times 10^7$	0.5 ( $\text{Cl}^-$ )	32	-1.38	$10 \times 10^7$	
$\text{Eu}^{3+}$	$\text{Ru}(4,7\text{-}(\text{CH}_3)_2\text{phen})_3^{3+}$	$4 \times 10^8$	2.7 ( $\text{Cl}^-$ )	<i>e</i>	-1.47	$3.4 \times 10^8$	
	$^*\text{Ru}(\text{phen})_3^{2+}$	$\sim 1 \times 10^5$	2.7 ( $\text{Cl}^-$ )	<i>e</i>	-0.49	$\sim 7 \times 10^4$	
	$^*\text{Ru}(5\text{-CH}_3\text{phen})_3^{2+}$	$4.2 \times 10^5$	2.7 ( $\text{Cl}^-$ )	<i>e</i>	-0.52	$2.9 \times 10^5$	
	$^*\text{Ru}(5,6\text{-}(\text{CH}_3)_2\text{phen})_3^{2+}$	$7.5 \times 10^5$	2.7 ( $\text{Cl}^-$ )	<i>e</i>	-0.55	$5.2 \times 10^5$	
	$^*\text{Ru}(4,4'\text{-}(\text{CH}_3)_2\text{bpy})_3^{2+}$	$\sim 5 \times 10^5$	2.7 ( $\text{Cl}^-$ )	<i>e</i>	-0.56	$\sim 3.5 \times 10^5$	
	$^*\text{Ru}(4,7\text{-}(\text{CH}_3)_2\text{phen})_3^{2+}$	$2.1 \times 10^6$	2.7 ( $\text{Cl}^-$ )	<i>e</i>	-0.63	$1.5 \times 10^6$	
	$\text{Ru}(5\text{-Clphen})_3^+$	$1.6 \times 10^7$	0.5 ( $\text{Cl}^-$ )	32	-0.77	$1.3 \times 10^7$	
	$\text{Ru}(\text{bpy})_3^+$	$2.7 \times 10^7$	0.5 ( $\text{Cl}^-$ )	32	-0.90	$2.3 \times 10^7$	
	$\text{Ru}(\text{phen})_3^+$	$5.2 \times 10^7$	0.5 ( $\text{Cl}^-$ )	32	-0.98	$4.3 \times 10^7$	
	$\text{Ru}(4,4'\text{-CH}_3)_2\text{bpy})_3^+$	$4.5 \times 10^7$	0.5 ( $\text{Cl}^-$ )	32	-0.99	$3.7 \times 10^7$	
	$\text{Ru}(4,7\text{-}(\text{CH}_3)_2\text{phen})_3^+$	$5.7 \times 10^7$	0.5 ( $\text{Cl}^-$ )	32	-1.09	$4.7 \times 10^7$	
$\text{Fe}^{2+}$	$\text{Os}(5,5'\text{-}(\text{CH}_3)_2\text{bpy})_3^{3+}$	$1.0 \times 10^3$ <i>f</i>	1.5 ( $\text{SO}_4^{2-}$ )	<i>g</i>	+0.01	$1.05 \times 10^3$	
	$\text{Os}(\text{bpy})_3^{3+}$	$1.4 \times 10^4$ <i>f</i>	1.5 ( $\text{SO}_4^{2-}$ )	<i>g</i>	-0.08	$1.5 \times 10^4$	
	$\text{Os}(\text{phen})_3^{3+}$	$1.1 \times 10^4$ <i>f</i>	1.5 ( $\text{SO}_4^{2-}$ )	<i>g</i>	-0.08	$1.2 \times 10^4$	
	$\text{Os}(5\text{-Clphen})_3^{3+}$	$7.0 \times 10^4$ <i>f</i>	1.5 ( $\text{SO}_4^{2-}$ )	<i>g</i>	-0.19	$7.4 \times 10^4$	
	$\text{Fe}(4,4'\text{-}(\text{CH}_3)_2\text{bpy})_3^{3+}$	$5.9 \times 10^3$	1.5 ( $\text{SO}_4^{2-}$ )	<i>h</i>	-0.21	$6.2 \times 10^3$	
	$\text{Fe}(5,6\text{-}(\text{CH}_3)_2\text{phen})_3^{3+}$	$6.9 \times 10^4$	1.5 ( $\text{SO}_4^{2-}$ )	<i>h</i>	-0.23	$7.3 \times 10^4$	
	$\text{Fe}(\text{bpy})_3^{3+}$	$2.2 \times 10^5$	1.5 ( $\text{SO}_4^{2-}$ )	<i>h</i>	-0.23	$2.3 \times 10^5$	
	$\text{Fe}(5\text{-CH}_3\text{phen})_3^{3+}$	$1.5 \times 10^5$	1.5 ( $\text{SO}_4^{2-}$ )	<i>h</i>	-0.28	$1.6 \times 10^5$	
	$\text{Ru}(3,4,7,8\text{-}(\text{CH}_3)_4\text{phen})_3^{3+}$	$6.1 \times 10^4$	1.5 ( $\text{SO}_4^{2-}$ )	<i>e</i>	-0.28	$6.4 \times 10^4$	
	$\text{Fe}(\text{phen})_3^{3+}$	$3.0 \times 10^5$	1.5 ( $\text{SO}_4^{2-}$ )	<i>h</i>	-0.32	$3.2 \times 10^5$	
	$\text{Ru}(3,5,6,8\text{-}(\text{CH}_3)_4\text{phen})_3^{3+}$	$2.7 \times 10^5$	1.5 ( $\text{SO}_4^{2-}$ )	<i>e</i>	-0.35	$2.8 \times 10^5$	
	$\text{Ru}(4,7\text{-}(\text{CH}_3)_2\text{phen})_3^{3+}$	$3.4 \times 10^5$	1.5 ( $\text{SO}_4^{2-}$ )	<i>e</i>	-0.35	$3.6 \times 10^5$	
	$\text{Ru}(4,4'\text{-}(\text{CH}_3)_2\text{bpy})_3^{3+}$	$2.1 \times 10^5$	1.5 ( $\text{SO}_4^{2-}$ )	<i>e</i>	-0.36	$2.2 \times 10^5$	
	$\text{Fe}(5\text{-Clphen})_3^{3+}$	$1.5 \times 10^6$	1.5 ( $\text{SO}_4^{2-}$ )	<i>h</i>	-0.38	$1.6 \times 10^6$	
	$\text{Ru}(5,5'\text{-}(\text{CH}_3)_2\text{bpy})_3^{3+}$	$6.0 \times 10^5$ <i>f</i>	1.5 ( $\text{SO}_4^{2-}$ )	<i>g</i>	-0.42	$6.3 \times 10^5$	
	$\text{Ru}(5,6\text{-}(\text{CH}_3)_2\text{phen})_3^{3+}$	$1.8 \times 10^6$	1.5 ( $\text{SO}_4^{2-}$ )	<i>e</i>	-0.46	$1.9 \times 10^6$	
	$\text{Ru}(5\text{-CH}_3\text{phen})_3^{3+}$	$3.0 \times 10^6$	1.5 ( $\text{SO}_4^{2-}$ )	<i>e</i>	-0.49	$3.2 \times 10^6$	
	$^*\text{Cr}(4,7\text{-}(\text{CH}_3)_2\text{phen})_3^{3+}$	$8.9 \times 10^5$	3.0 ( $\text{SO}_4^{2-}$ )	<i>i</i>	-0.49	$7.7 \times 10^5$	
	$^*\text{Cr}(4,4'\text{-}(\text{CH}_3)_2\text{bpy})_3^{3+}$	$8.2 \times 10^5$	3.0 ( $\text{SO}_4^{2-}$ )	<i>i</i>	-0.51	$7.1 \times 10^5$	
	$\text{Fe}(5\text{-NO}_2\text{phen})_3^{3+}$	$1.1 \times 10^6$	0.5 ( $\text{ClO}_4^-$ )	<i>h</i>	-0.51	$1.7 \times 10^6$	
	$\text{Ru}(\text{bpy})_3^{3+}$	$4.9 \times 10^6$	1.5 ( $\text{SO}_4^{2-}$ )	<i>e</i>	-0.52	$5.2 \times 10^6$	
	$\text{Ru}(5\text{-C}_6\text{H}_5\text{phen})_3^{3+}$	$4.6 \times 10^6$	1.5 ( $\text{SO}_4^{2-}$ )	<i>e</i>	-0.52	$4.8 \times 10^6$	
	$\text{Ru}(\text{phen})_3^{3+}$	$5.6 \times 10^6$	1.5 ( $\text{SO}_4^{2-}$ )	<i>e</i>	-0.52	$5.9 \times 10^6$	
	$\text{Ru}(5\text{-Clphen})_3^{3+}$	$2.2 \times 10^7$	1.5 ( $\text{SO}_4^{2-}$ )	<i>e</i>	-0.62	$2.3 \times 10^7$	
	$^*\text{Cr}(5\text{-CH}_3\text{phen})_3^{3+}$	$1.0 \times 10^7$	3.0 ( $\text{SO}_4^{2-}$ )	<i>i</i>	-0.65	$8.6 \times 10^6$	
	$^*\text{Cr}(\text{phen})_3^{3+}$	$1.5 \times 10^7$	3.0 ( $\text{SO}_4^{2-}$ )	<i>i</i>	-0.68	$1.3 \times 10^7$	
	$^*\text{Cr}(\text{bpy})_3^{3+}$	$1.6 \times 10^7$	3.0 ( $\text{SO}_4^{2-}$ )	<i>i</i>	-0.70	$1.4 \times 10^7$	
	$^*\text{Cr}(\text{bpy})_3^{3+}$	$4.1 \times 10^7$ <i>f</i>	1.0 ( $\text{SO}_4^{2-}$ )	<i>j</i>	-0.70	$4.9 \times 10^7$	
	$^*\text{Cr}(5\text{-Clphen})_3^{3+}$	$4.8 \times 10^7$	3.0 ( $\text{SO}_4^{2-}$ )	<i>i</i>	-0.79	$4.1 \times 10^7$	
	$\text{Fe}^{3+}$	$\text{Ru}(\text{NH}_3)_4\text{bpy}^{2+}$	$7.2 \times 10^3$	1.0 ( $\text{ClO}_4^-$ )	15	-0.22	$1.6 \times 10^5$ <i>k</i>
		$\text{Ru}(\text{NH}_3)_5\text{isn}^{2+}$	$2.6 \times 10^4$	1.0 ( $\text{CF}_3\text{SO}_3^-$ )	13	-0.36	$2.4 \times 10^6$ <i>k</i>
		$\text{Ru}(\text{NH}_3)_5\text{nic}^{2+}$	$2.9 \times 10^4$	1.0 ( $\text{CF}_3\text{SO}_3^-$ )	13	-0.38	$2.5 \times 10^6$ <i>k</i>
$\text{Ru}(\text{NH}_3)_5\text{py}^{2+}$		$7.8 \times 10^4$	1.0 ( $\text{CF}_3\text{SO}_3^-$ )	13	-0.44	$5.1 \times 10^6$ <i>k</i>	
$\text{Ru}(\text{NH}_3)_6^{2+}$		$3.4 \times 10^5$	0.1 ( $\text{ClO}_4^-$ )	15	-0.67	$4.5 \times 10^8$ <i>k</i>	
$\text{Cr}(\text{bpy})_3^{2+}$		$7.3 \times 10^8$ <i>f</i>	0.2 ( $\text{SO}_4^{2-}$ )	<i>j</i>	-1.0	$1.6 \times 10^9$	
$\text{Cr}(5,6\text{-}(\text{CH}_3)_2\text{phen})_3^{2+}$		$4.8 \times 10^8$	0.15 ( $\text{SO}_4^{2-}$ )	<i>l</i>	-1.12	$1.2 \times 10^9$	
$\text{Cr}(4,4'\text{-}(\text{CH}_3)_2\text{bpy})_3^{2+}$		$7.0 \times 10^8$	0.15 ( $\text{SO}_4^{2-}$ )	<i>l</i>	-1.19	$1.7 \times 10^9$	
$\text{Cr}(4,7\text{-}(\text{CH}_3)_2\text{phen})_3^{2+}$		$7.1 \times 10^8$	0.15 ( $\text{SO}_4^{2-}$ )	<i>l</i>	-1.23	$1.7 \times 10^9$	
$^*\text{Ru}(5\text{-Brphen})_3^{2+}$		$2.3 \times 10^9$	1.5 ( $\text{SO}_4^{2-}$ )	<i>e</i>	-1.50	$2.4 \times 10^9$	
$^*\text{Ru}(5\text{-Clphen})_3^{2+}$		$2.3 \times 10^9$	1.5 ( $\text{SO}_4^{2-}$ )	<i>e</i>	-1.51	$2.4 \times 10^9$	
$^*\text{Ru}(\text{bpy})_3^{2+}$		$2.7 \times 10^9$	1.5 ( $\text{SO}_4^{2-}$ )	<i>e</i>	-1.58	$2.8 \times 10^9$	
$^*\text{Os}(5\text{-Clphen})_3^{2+}$		$3.2 \times 10^9$ <i>f</i>	1.5 ( $\text{SO}_4^{2-}$ )	<i>g</i>	-1.59	$3.3 \times 10^9$	
$^*\text{Ru}(5\text{-C}_6\text{H}_5\text{phen})_3^{2+}$		$2.7 \times 10^9$	1.5 ( $\text{SO}_4^{2-}$ )	<i>e</i>	-1.61	$2.8 \times 10^9$	
$^*\text{Ru}(\text{phen})_3^{2+}$		$2.8 \times 10^9$	1.5 ( $\text{SO}_4^{2-}$ )	<i>e</i>	-1.61	$2.9 \times 10^9$	
$^*\text{Ru}(5\text{-CH}_3\text{phen})_3^{2+}$		$2.6 \times 10^9$	1.5 ( $\text{SO}_4^{2-}$ )	<i>e</i>	-1.64	$2.7 \times 10^9$	
$^*\text{Ru}(5,6\text{-}(\text{CH}_3)_2\text{phen})_3^{2+}$		$2.6 \times 10^9$	1.5 ( $\text{SO}_4^{2-}$ )	<i>e</i>	-1.67	$2.7 \times 10^9$	
$^*\text{Ru}(4,4'\text{-}(\text{CH}_3)_2\text{bpy})_3^{2+}$		$2.9 \times 10^9$	1.5 ( $\text{SO}_4^{2-}$ )	<i>e</i>	-1.68	$3.0 \times 10^9$	
$^*\text{Os}(\text{phen})_3^{2+}$		$4.0 \times 10^9$ <i>f</i>	1.5 ( $\text{SO}_4^{2-}$ )	<i>g</i>	-1.70	$4.1 \times 10^9$	
$^*\text{Os}(\text{bpy})_3^{2+}$		$5.5 \times 10^9$ <i>f</i>	1.5 ( $\text{SO}_4^{2-}$ )	<i>g</i>	-1.70	$5.6 \times 10^9$	
$^*\text{Ru}(4,7\text{-}(\text{CH}_3)_2\text{phen})_3^{2+}$		$3.0 \times 10^9$	1.5 ( $\text{SO}_4^{2-}$ )	<i>e</i>	-1.75	$3.1 \times 10^9$	
$^*\text{Ru}(3,5,6,8\text{-}(\text{CH}_3)_4\text{phen})_3^{2+}$		$2.5 \times 10^9$	1.5 ( $\text{SO}_4^{2-}$ )	<i>e</i>	-1.78	$2.6 \times 10^9$	
$^*\text{Ru}(3,4,7,8\text{-}(\text{CH}_3)_4\text{phen})_3^{2+}$		$3.4 \times 10^9$	1.5 ( $\text{SO}_4^{2-}$ )	<i>e</i>	-1.85	$3.5 \times 10^9$	
$\text{Ru}(\text{NH}_3)_6^{2+}$	$\text{Ru}(\text{NH}_3)_6^{3+}$	$4 \times 10^3$	0.1 ( $\text{ClO}_4^-$ )	13	0	$1.4 \times 10^7$ <i>k</i>	
	$\text{Ru}(\text{NH}_3)_5\text{py}^{3+}$	$7.2 \times 10^5$	0.1 ( $\text{NO}_3^-$ )	<i>m</i>	-0.23	$4.4 \times 10^8$ <i>k</i>	
	$^*\text{Os}(5\text{-Clphen})_3^{2+}$	$1 \times 10^9$	0.2 ( $\text{CH}_3\text{COO}^-$ )	34	-0.65	$1.3 \times 10^9$	
	$^*\text{Ru}(\text{bpy})_3^{2+}$	$2.4 \times 10^9$	0.2 ( $\text{CH}_3\text{COO}^-$ )	34	-0.77	$3.1 \times 10^9$	
	$\text{Ru}(\text{bpy})_3^{3+}$	$3.7 \times 10^9$ <i>f</i>	1.0 ( $\text{CF}_3\text{CO}_2^-$ )	<i>n</i>	-1.19	$4.1 \times 10^9$	

Table I (Continued)

A <sub>1</sub>	redox partner, A <sub>2</sub>	k <sub>12</sub> <sup>obsd a</sup>	μ, M (anion)	ref	ΔG, <sup>b</sup> eV	k <sub>12</sub> <sup>corr c</sup>
Ru(NH <sub>3</sub> ) <sub>6</sub> <sup>3+</sup>	*Os(bpy) <sub>3</sub> <sup>2+</sup>	4.8 × 10 <sup>9</sup>	0.5 (Cl <sup>-</sup> )	o	-0.89	5.8 × 10 <sup>9</sup>
	*Ru(bpy) <sub>3</sub> <sup>2+</sup>	2.7 × 10 <sup>9</sup>	0.5 (Cl <sup>-</sup> )	o	-0.91	3.7 × 10 <sup>9</sup>
	Ru(bpy) <sub>3</sub> <sup>+</sup>	4.7 × 10 <sup>9</sup>	0.5 (Cl <sup>-</sup> )	34	-1.35	4.3 × 10 <sup>9</sup>

<sup>a</sup> Aqueous solution, 25 °C, unless otherwise noted. <sup>b</sup> Free energy change of the electron-transfer step calculated from the standard redox potentials of the reaction partners neglecting the work term ( $-4 \times 10^{-3}$  eV). The following values have been used for the A<sub>1</sub> species:  $E^\circ(\text{Eu}^{3+/2+}) = -0.38$  V (1 M NaClO<sub>4</sub>);<sup>43</sup>  $E^\circ(\text{Fe}^{3+/2+}) = +0.74$  V;<sup>13</sup>  $E^\circ(\text{Ru}(\text{NH}_3)_6^{3+/2+}) = +0.067$  V.<sup>13</sup> The standard potentials for the A<sub>2</sub> species have been taken from ref 13, 15, 18, 32, and 34 and from: Ford-Smith, M. H.; Sutin, N. *J. Am. Chem. Soc.* 1961, 83, 1830. Lin, C.-T.; Böttcher, W.; Chou, M.; Creutz, C.; Sutin, N. *Ibid.* 1976, 98, 6536. Ohsawa, Y.; Saji, T.; and Aoyagui, S. *J. Electroanal. Chem.* 1980, 106, 327. <sup>c</sup> Homogenized according to Appendix II for differences in encounter distance, charge product, and ionic strength. <sup>d</sup> Faraggi, M.; Feder, A. *Inorg. Chem.* 1973, 12, 236. <sup>e</sup> Lin, C.-T.; Böttcher, W.; Chou, M.; Creutz, C.; Sutin, N. *J. Am. Chem. Soc.* 1976, 98, 6536. <sup>f</sup> Room temperature. <sup>g</sup> Ohsawa, Y.; Saji, T.; Aoyagui, S. *J. Electroanal. Chem.* 1980, 106, 327. <sup>h</sup> Ford-Smith, M. H.; Sutin, N. *J. Am. Chem. Soc.* 1961, 83, 1830. <sup>i</sup> Brunschwag, B.; Sutin, N. *Ibid.* 1978, 100, 7568. <sup>j</sup> Ballardini, R.; Varani, G.; Scandola, F.; Balzani, V. *Ibid.* 1976, 98, 7432. <sup>k</sup> Corrected also for differences in intrinsic barriers (Appendix I). <sup>l</sup> Serpone, N.; Emmi, S.; private communication. <sup>m</sup> Miralles, A. J.; Armstrong, R. E.; Haim, A. *J. Am. Chem. Soc.* 1977, 99, 1416. <sup>n</sup> Bock, C. R.; Meyer, T. J.; Whitten, D. G. *Ibid.* 1974, 96, 4710. <sup>o</sup> Lin, C.-T.; Sutin, N. *J. Phys. Chem.* 1976, 80, 97.

For the Ru(NH<sub>3</sub>)<sub>6</sub><sup>n+</sup> reactions (Figure 2), the rate constant approaches the diffusion value for slightly negative ΔG values. As we have seen in the previous section, this behavior is expected for adiabatic or nearly adiabatic<sup>24</sup> reactions having a small intrinsic barrier. The curve drawn through the points in Figure 2 has been obtained from eq 7 and 11 for an intrinsic barrier ΔG<sub>11</sub> = 10.6 kcal/mol for the Ru(NH<sub>3</sub>)<sub>6</sub><sup>3+/2+</sup> exchange.<sup>36</sup>

For the Fe<sup>n+</sup> reactions (Figure 2), the nonlinear part of the plot is considerably wider than for Ru(NH<sub>3</sub>)<sub>6</sub><sup>n+</sup>, as expected (see Figure 1) for a species having a higher intrinsic barrier. The curve drawn through the points has been obtained from eq 7 and 11 with ΔG\* = 17.4 kcal/mol for the Fe<sup>3+/2+</sup> exchange.<sup>38</sup>

For the reactions involving the europium ions the log k<sub>12</sub><sup>corr</sup> vs. ΔG plot (Figure 3) has a rather peculiar aspect. Prior to any analysis of this plot, the actual nature of the europium species present in the solution should be considered in view of the high Cl<sup>-</sup> concentrations used. For Eu(II) there is no problem because it is not expected to form complexes with Cl<sup>-</sup> ions. The presence of important pathways involving halide complexes in the electrochemical oxidation of Eu<sup>2+</sup> has in fact been excluded.<sup>39</sup> For Eu(III) the formation constant of EuCl<sub>2</sub><sup>+</sup> is ~1 M<sup>-1</sup>.<sup>40,41</sup> This means that in the experimental conditions in which the Eu(III) data were obtained (0.5 or 1.8 M Cl<sup>-</sup>, ~0.1 M Eu(III)) the amount of uncomplexed aquo ion varied from 60 to 30%, the remaining Eu(III) being present as EuCl<sub>2</sub><sup>+</sup>. However, thermodynamic,<sup>40,42</sup> electrochemical,<sup>43</sup> and structural<sup>44</sup> data show that the EuCl<sub>2</sub><sup>+</sup> species is an outer-sphere ion pair. In particular, Weaver and Anson<sup>43,45</sup> have shown that the formal potentials of the Eu(III)/Eu(II) couple in 1 M KCl or NaClO<sub>4</sub> only differ by 8 mV and that ion pairing with Cl<sup>-</sup> produces little or no effect on the electrochemical reactivity of the simple aquated cation at negatively charged electrodes. However, one cannot rule out that ion pairing may enhance the reactivity of Eu<sup>3+</sup> when the reaction partner is, as in our case, a cationic species. In such a case the literature data for Eu<sup>3+</sup> (Figure 3) would represent upper limiting values for the reactivity of the aquo Eu<sup>3+</sup> ion.

A very important feature of the plot shown in Figure 3 is that the rate constants are much lower than the diffusion constant even for very negative ΔG values. This behavior could in principle be

due to a very high intrinsic barrier. In such a case, however, the log k<sub>12</sub><sup>corr</sup> vs. ΔG plot would be a smooth curve with a (negative) slope continuously increasing with increasing ΔG to reach the value  $-0.5 [1/(2.3RT)]$  at ΔG = 0 and  $-1/(2.3RT)$  for ΔG ≥ 4ΔG\*(0), i.e., for very positive ΔG values. This does not seem to be the case of the plot of Figure 3. For Eu<sup>2+</sup>, where a wider ΔG range has been explored, the plot is suggestive of a stepwise behavior or at least of an increase in the slope with decreasing ΔG.<sup>46</sup> For Eu<sup>3+</sup> the plot does not show steps but its slope approaches the limiting  $-1/(2.3RT)$  value for negative ΔG.

Admittedly, some details of the plot of Figure 3 could be a consequence of errors in the experimental data. However, the fact remains that for the same ΔG value the rate constants are much lower for europium than for iron. If the slowness of Eu<sup>2+</sup> oxidation were only attributed to reorganization reasons, a ΔG\*<sub>11</sub> value of about 30 kcal/mol would be obtained. With the assumption that the same κ value used to fit the iron data,<sup>38</sup> the Eu<sup>3+/2+</sup> reorganization barrier (~26 kcal/mol) would still be much higher than that of the Fe<sup>3+/2+</sup> couple. This is implausible because, as first observed by Taube,<sup>11</sup> the europium ions, being larger than the iron ions, are expected to have a smaller outer- and inner-sphere contribution to the intrinsic barrier. It can be argued<sup>47</sup> that the Eu<sup>3+/2+</sup> couple may have an anomalously high intrinsic barrier because Eu<sup>3+</sup> and Eu<sup>2+</sup> coordinate a different number of water molecules. This argument, however, does not seem plausible because of the very weak bonding of water to europium. This is demonstrated by the very fast exchange rate of the inner-sphere water molecules<sup>48,49</sup> and by the fact that the hydration numbers of lanthanides are essentially determined by the radius of the ion.<sup>44,50</sup> An upper limit for the contribution of the change in coordination number to the intrinsic barrier is in fact estimated to be ~5 kcal/mol.<sup>51</sup> Weaver et al.<sup>53</sup> have recently

(46) Recall that, as previously mentioned, the points corresponding to Eu<sup>2+</sup> oxidation by Ru(NH<sub>3</sub>)<sub>6</sub><sup>3+</sup> and Ru(NH<sub>3</sub>)<sub>6</sub>py<sup>3+</sup> would become higher than those shown in Figure 3 after correction for the intrinsic barrier of the partner.

(47) This argument has been advanced by a reviewer.

(48) Basolo, F.; Pearson, R. G. "Mechanisms of Inorganic Reactions"; Wiley-Interscience: New York, 1967; Chapter 3.

(49) Geier, G. *Ber. Bunsenges. Phys. Chem.* 1965, 69, 617.

(50) Kamo, H.; Akama, Y. *Chem. Phys. Lett.* 1980, 72, 181.

(51) This estimate is obtained as follows. An upper limit for the energy needed for the release of a water molecule from Eu<sup>2+</sup> is given by the activation energy of the water-exchange reaction. The rate constant of water exchange for Eu<sup>2+</sup> is not known, but it must certainly be higher than that of the smaller and more charged Gd<sup>3+</sup> ion ( $2 \times 10^9$  s<sup>-1</sup>).<sup>52</sup> Taking a preexponential factor of  $10^{13}$  s<sup>-1</sup>, the activation energy of water exchange of Gd<sup>3+</sup> results to be ~5 kcal/mol. For the larger and less charged Eu<sup>2+</sup> ion, a value of 2–3 kcal/mol seems appropriate. Thus, assuming a change of two in the coordination number (which is certainly a conservative estimate on the basis of the Eu<sup>2+</sup> radius and the trend shown in Figure 7 of ref 44), we estimate the contribution to the intrinsic barrier to be lower than ~5 kcal/mol. This argument emphasizes the point that the energy barriers caused by changes in coordination number or more generally by large ligand displacements depend more on bond energy than on bond length changes.

(52) Reference 48, p 152.

(53) Yee, E. L.; Cave, R. J.; Guyer, K. L.; Tuma, P. D.; Weaver, M. J. *J. Am. Chem. Soc.* 1979, 101, 1131.

(36) The parameters used in the calculation are as follows: κ = 1; k<sub>d</sub> = 4.5 × 10<sup>9</sup> M<sup>-1</sup> s<sup>-1</sup>; k<sub>-d</sub> = 2.8 × 10<sup>9</sup> s<sup>-1</sup>; k'<sub>-d</sub> = 2.6 × 10<sup>9</sup> s<sup>-1</sup>; ΔG<sub>22</sub> = 6 kcal/mol, obtained from k<sub>22</sub> = (k<sub>d</sub>/k<sub>-d</sub>)κ(kT/h) exp(-ΔG<sub>22</sub>/RT) by using k<sub>22</sub> = 4.2 × 10<sup>8</sup> M<sup>-1</sup> s<sup>-1</sup> (μ = 0.1)<sup>37</sup> corrected for diffusion<sup>37</sup> and ionic strength (Appendix II).

(37) Young, R. C.; Keene, F. R.; Meyer, T. J. *J. Am. Chem. Soc.* 1977, 99, 2468.

(38) The parameters used are the same as those in ref 36 except for κ which has been taken as 5 × 10<sup>-2</sup> from ref 13.

(39) Weaver, M. J.; Anson, F. C. *J. Electroanal. Chem.* 1977, 84, 47.

(40) Choppin, G. R.; Unrein, P. J. *J. Inorg. Nucl. Chem.* 1963, 25, 387.

(41) Khopkar, P. K.; Narayanankutty, P. *J. Inorg. Nucl. Chem.* 1971, 33, 495.

(42) Choppin, G. R.; Ketels, J. *J. Inorg. Nucl. Chem.* 1965, 27, 1335.

(43) Weaver, M. J.; Anson, F. C. *J. Electroanal. Chem.* 1975, 65, 737.

(44) Habenschuss, A.; Spedding, F. H. *J. Chem. Phys.* 1980, 73, 442.

(45) Weaver, M. J.; Anson, F. C. *J. Electroanal. Chem.* 1975, 65, 711.

found that  $\Delta S_{rc}^{\circ}$  (the entropy difference between ions forming a  $M^{3+/2+}$  redox couple) is much larger for aquo ions than for amine complexes. This finding, which has been attributed to the higher "structure-making" ability of the tripositive aquo ions toward the surrounding water molecules, has also been considered as a signal indicating that in the aquo ions additional solvent reorganization may be required besides that considered in the simple dielectric continuum model. Although the  $Eu^{3+/2+}$  and  $Fe^{3+/2+}$  couples have about the same  $\Delta S_{rc}^{\circ}$  value, we believe that such an additional contribution would be larger for the smaller and more strongly bound (and thus, better "structure-making")  $Fe^{3+}$  species.<sup>54</sup> This is consistent with the finding that substituting  $D_2O$  for  $H_2O$  as solvent causes a much smaller effect on the formal potential of the  $Eu^{3+/2+}$  couple than on that of the  $Fe^{3+/2+}$  couple.<sup>56,57</sup> In conclusion, the  $Eu^{3+/2+}$  couple may have a *small* additional contribution to the reorganization barrier due to the change in coordination number, but its inner- and outer-sphere contributions are certainly smaller than those of the  $Fe^{3+/2+}$  couple. Thus, it seems safe to conclude that the overall intrinsic barrier of the  $Eu^{3+/2+}$  couple cannot be larger than that of the  $Fe^{3+/2+}$  couple and that the much lower rate constants observed for the europium ions must have their origin in rate saturation effects. Very recently Weaver and Yee<sup>58</sup> have discussed the presence of large unfavorable work terms required to form the bimolecular collision complex prior to electron transfer. These terms, which would be particularly important for aquo ions, are associated to the need to reorientate solvating water molecules in order to form the highly charged collision complex. A similar problem had been previously discussed by Marcus<sup>59</sup> and other authors<sup>60</sup> for proton-transfer reactions. The inclusion of such a work term would introduce a rate saturation effect and could thus explain low plateau values in the  $\log k_{12}^{corr}$  vs.  $\Delta G$  plots. This effect, however, is not expected to be larger for europium than for iron and should also cause rate saturation for the iron reaction at  $k_{12}^{corr}$  values much lower than those experimentally found (Figure 3). Thus we are left with nonadiabaticity as the only plausible explanation for the lower rate constants of europium reactions compared to the iron ones.

The assumption that the redox processes of europium ions exhibit a nonadiabatic behavior can account not only for the lower rate constants compared to those for iron but also for the peculiar aspect of the europium plot (Figure 3). When a reaction is very slow for adiabatic reasons, it is predicted that the rate constant tends to a lower than diffusion plateau value for large and negative  $\Delta G$  values (e.g., curve c in Figure 1). At the same time, it may also be expected that thermodynamically less favorable but kinetically more efficient channels come into play with increasing exoergonicity. In such a case, the  $\log k_{12}^{corr}$  vs.  $\Delta G$  plot cannot be a smooth curve with slope continuously decreasing with decreasing  $\Delta G$ , as one would expect on the basis of eq 7 and 11. Rather, one can expect a sudden increase in the slope when, as  $\Delta G$  decreases, a kinetically more efficient reaction channel becomes thermodynamically allowed and thus takes up the process which would otherwise display rate saturation. In this view, the data for  $Eu^{2+}$  oxidation are indicative of a reaction that approaches rate saturation for moderately negative  $\Delta G$  values and a new reaction channel which comes into play at about  $-1$  eV.<sup>46</sup> Similarly, the data for  $Eu^{3+}$  reduction may be interpreted as belonging to a reaction channel arising at about  $-0.5$  eV. As we will discuss later, the new channels that may come into play at high exoergonicity are in fact expected to be different for  $Eu^{2+}$  reduction or  $Eu^{3+}$  oxidation, and this would account for the very peculiar fact that the data for  $Eu^{2+}$  oxidation do not lie on the same curve

as those for  $Eu^{3+}$  reduction.<sup>61</sup> The paucity of data (especially at small negative  $\Delta G$  values) does not allow one to obtain a definite estimate of the adiabaticity coefficient for the ground-state outer-sphere electron-transfer process for which the free energy scale of Figure 3 is appropriate. However, a plausible value for a plateau in the weakly exoergonic region for  $Eu^{2+}$  oxidation seems to be of the order of  $10^6 M^{-1} s^{-1}$ , which means that the adiabaticity coefficient  $\kappa$  should be  $\sim 10^{-6}$ .

In principle, the higher rate constants for  $Eu(III)$  reduction could also be explained on the basis of the previously mentioned possibility that the reduction of  $EuCl_2^{2+}$  is much faster than that of the  $Eu^{3+}$  aquo ion. This explanation, however, does not seem to be supported by the experimental data. In such a case, in fact, the data for  $Eu(III)$  reduction in Figure 3, after correction for the fraction of  $EuCl_2^{2+}$  actually present in the solution, should lie on a monotonous smooth curve reaching a slope of  $-0.5/(2.3RT)$  at  $\Delta G$  close to zero. As mentioned above, however, the  $Eu(III)$  plot seems already to exhibit a much steeper slope at  $\sim -0.5$  eV. Correction for the different concentrations of  $Cl^-$  used in the experiments would even reinforce this trend.

As previously mentioned, Creutz<sup>32</sup> had already observed that the reactions of  $Eu^{2+}$  with  $*Ru(LL)_3^{2+}$  exhibit a different free energy dependence than the reactions of  $Eu^{3+}$  with  $Ru(LL)_3^{3+}$ . She<sup>32</sup> also noticed that these reactions involve different orbitals in the  $Ru(LL)_3^{n+}$  species. Reductive quenching involves a "metal"  $t_{2g}$  acceptor orbital while the reactions of  $Eu^{3+}$  with  $Ru(LL)_3^{3+}$  (as well as the oxidative quenching of  $*Ru(LL)_3^{2+}$ ) involve a "ligand"  $\pi^*$ -donor orbital. Thus, reductive quenching could exhibit nonadiabatic behavior owing to poor overlap of the  $Eu^{2+}$  f orbital with the  $*Ru(LL)_3^{2+}$   $t_{2g}$  "metal" orbital, whereas in the reactions of  $Eu^{3+}$  a better orbital overlap might be expected between the europium f orbital and the "ligand"  $\pi^*$  orbital, leading to adiabatic behavior. However Creutz<sup>32</sup> also observed that such a model does not account for the unusual driving-force dependence of the  $Eu^{3+}$  reactions. We believe that although the nature of the orbital involved in the reaction partner may play some role, it cannot be responsible for the observed behavior because in the  $Ru(bpy)_3^{n+}$  species there is extensive mixing between "metal" and "ligand" orbitals. Moreover, the reactions of  $Cu^+$  with  $Ru(LL)_3^{3+}$  (where a "metal"  $t_{2g}$  acceptor orbital is involved) are *faster* than those of  $Cu^{2+}$  with  $*Ru(LL)_3^{2+}$  or  $Ru(LL)_3^{3+}$  (which involve a  $\pi^*$ -donor orbital) for the same  $\Delta G$  values (see Figure 4 of ref 62), showing that the reason for the different behavior in oxidation or reduction of both europium and copper aquo ions has to be found in the intrinsic properties of these species.

**Theoretical Expectations Concerning the Rate Constants.** An estimate of the nonadiabaticity of the redox reactions of europium ions can be given by means of theoretical arguments based on spectroscopic information. These reactions involving the ground states of  $Eu^{3+}$  and  $Eu^{2+}$  ions imply the transfer of an electron to or from a 4f orbital which is heavily shielded from interaction with the orbitals of the reaction partner not only by solvent (or ligand) molecules but also by the outermost filled 5s and 5p metal orbitals. The atomic character of the f orbitals is shown by the insensitivity of the energy of the f-f excited states to the ligand field and by the very narrow width of the f-f bands.<sup>63,64</sup> Therefore the electronic matrix element coupling the initial and the final states of the electron transfer to or from ground-state europium ions is expected to be very small, leading to a vanishingly small value of the adiabaticity coefficient.

An estimate of the strength of this coupling requires consideration of contributions other than f orbital interactions and calls for a detailed description of the states of  $Eu^{3+}$  and  $Eu^{2+}$ . Although to a first approximation each state is described in terms of a pure

(54) A crude correlation between  $\Delta S_{rc}^{\circ}$  and outer-sphere intrinsic barrier is observed for some redox couples, but it has been pointed out that it may be somewhat deceiving.<sup>55</sup>

(55) Sutin, N.; Weaver, M. J.; Yee, E. L. *Inorg. Chem.* **1980**, *19*, 1096.

(56) Weaver, M. J.; Nettles, S. M. *Inorg. Chem.* **1980**, *19*, 1641.

(57) In the original paper,<sup>56</sup> the smaller effect found for the  $Eu^{3+/2+}$  couple is suggested to be due to complications from the probable change in the number of coordinated aquo ligands between  $Eu^{3+}$  and  $Eu^{2+}$ .

(58) Weaver, M. J.; Yee, E. L. *Inorg. Chem.* **1980**, *19*, 1936.

(59) Marcus, R. A. *J. Phys. Chem.* **1968**, *72*, 891.

(60) Kresge, A. J. *Chem. Soc. Rev.* **1973**, *2*, 475.

(61) The fact that the data for  $Eu^{2+}$  oxidation do not lie on the same curve as those of  $Eu^{3+}$  reduction implies that the rates of  $Eu^{3+}$  reduction cannot be obtained from the potential of the  $Eu^{3+/2+}$  couple and the corresponding rates of  $Eu^{2+}$  oxidation (and vice versa), at least in the energy range considered here.

(62) Hoselton, M. A.; Lin, C. T.; Schwarz, M. A.; Sutin, N. *J. Am. Chem. Soc.* **1978**, *100*, 2383.

(63) Jorgensen, C. K. *Struct. Bonding (Berlin)* **1973**, *13*, 199.

(64) Streak, W.; Ballhausen, C. J. *Mol. Phys.* **1978**, *36*, 132.



electronic configuration, in reality it is represented by a linear combination of configurations because of the Coulombic interaction between metal and ligand electrons.<sup>64</sup> Thus, for example, the ground states of  $\text{Eu}^{3+}$  and  $\text{Eu}^{2+}$  contain, besides a dominant fraction of their respective lower energy configurations, a small fraction of f-d, charge transfer (CT), and ligand-centered configurations. This mixed character of the electronic states, which is considered responsible for the electronic dipole oscillator strength of the parity-forbidden f-f transitions,<sup>65,66</sup> is also expected to govern the electron-transfer processes to or from  $\text{Eu}^{3+}$  and  $\text{Eu}^{2+}$  ground states. In fact, the f-d and ligand-to-metal CT configurations, having an electron and a hole, respectively, available in an outer orbital, can interact very effectively with a redox partner.

Spectroscopic data and theoretical treatments show that f-d and ligand-to-metal CT excited configurations lie at relatively low energies in  $\text{Eu}^{2+}$  and  $\text{Eu}^{3+}$ , respectively.<sup>65</sup> Thus, to a first approximation the wave functions of the  $\text{Eu}^{2+}$  and  $\text{Eu}^{3+}$  ground states can be written as eq 13 and 13', where  $\Phi_0$  is the ground-state

$$\Psi_0(\text{Eu}^{2+}) = \Phi_0(\text{Eu}^{2+}) + \alpha\Phi_{f-d}(\text{Eu}^{2+}) \quad (13)$$

$$\Psi_0(\text{Eu}^{3+}) = \Phi_0(\text{Eu}^{3+}) + \beta\Phi_{CT}(\text{Eu}^{3+}) \quad (13')$$

configuration and  $\Phi_{f-d}$  and  $\Phi_{CT}$  represent the f-d and CT excited configurations. Following perturbation theory, the coefficients  $\alpha$  and  $\beta$  are given by eq 14 and 14', where  $H'$  represents a suitable,

$$\alpha = \frac{\langle \Phi_0(\text{Eu}^{2+}) | H' | \Phi_{f-d}(\text{Eu}^{2+}) \rangle}{E_0 - E_{f-d}} \quad (14)$$

$$\beta = \frac{\langle \Phi_0(\text{Eu}^{3+}) | H' | \Phi_{CT}(\text{Eu}^{3+}) \rangle}{E_0 - E_{CT}} \quad (14')$$

geometry-dependent, electronic interaction. Using eq 13 and 13' and their analogues for the excited states, the ratio between typical intensities of f-f and f-d (or CT) transitions is found to be  $\alpha^2$  (or  $\beta^2$ ).<sup>66</sup> In a similar way it can be shown that the electronic factor for a redox process involving  $\text{Eu}^{2+}$  (or  $\text{Eu}^{3+}$ ) in the ground state is  $\alpha^2$  (or  $\beta^2$ ) times that with  $\text{Eu}^{2+}$  (or  $\text{Eu}^{3+}$ ) in f-d (or CT) excited states.

The experimental intensities of the relevant spectroscopic transitions<sup>63,65,67</sup> suggest that  $\alpha^2 \approx \beta^2 \leq 10^{-5}$ . Thus, in the nonadiabatic regime the redox reactions of ground-state  $\text{Eu}^{2+}$  or  $\text{Eu}^{3+}$  are expected to have an electronic factor at least  $10^5$  times smaller than those of the f-d or CT excited states. With the assumption of a nearly adiabatic value  $k_e^0 \approx 10^{12} \text{ s}^{-1}$  for the frequency factor of the electron-transfer rate constant between an f-d or CT excited state with an adiabatic-type partner, a value of  $\leq 10^7 \text{ s}^{-1}$  is obtained for the frequency factor of the reactions involving the ground-state  $\text{Eu}^{2+}$  or  $\text{Eu}^{3+}$  ions with an adiabatic-type partner. Such an estimate is consistent with the conclusion drawn in the previous section of strongly nonadiabatic behavior of the ground-state  $\text{Eu}^{2+}$  and  $\text{Eu}^{3+}$  outer-sphere reactions and also supports the suggestion offered by Figure 3 that, at not too negative  $\Delta G$  values, the rate constants of such reactions tend to a plateau value of  $\sim 10^6 \text{ M}^{-1} \text{ s}^{-1}$ .<sup>68</sup>

As mentioned before, it is to be expected that other, electronically more efficient, channels become important at high exoergonicity when, with increasing driving force, the rate constant of an outer-sphere reaction tends to a lower than diffusion-controlled value because of nonadiabaticity. For example, outer-sphere reactions leading to excited states of the species under investigation may involve outer orbitals and thus may be much less nonadiabatic than the reaction leading to the ground state.

(65) Blasse, G. *Struct. Bonding (Berlin)* 1976, 26, 43.

(66) Actually, the ratio is smaller because f-f transitions borrow intensity mainly from ligand centered transitions.<sup>67</sup>

(67) Mason, S. F. *Struct. Bonding (Berlin)* 1980, 39, 43.

(68) The same arguments used above allow to rationalize the very small rate constant of the  $\text{Eu}^{3+}$ - $\text{Eu}^{2+}$  exchange ( $\leq 3 \times 10^{-5} \text{ M}^{-1} \text{ s}^{-1}$ ).<sup>30</sup> With use of wave functions (13) and (13') and the interaction operator  $1/r_{12}$ , it can be shown that this process is governed by an electron matrix element proportional to  $\alpha^2\beta^2$ . Accordingly, the adiabaticity factor for the exchange reaction is estimated to be  $\leq 10^{-10}$ .

Thus, when the process becomes sufficiently exoergonic to allow the formation of one of such excited states, the rate constant is expected to increase above the plateau of the nonadiabatic ground-state reaction. Moreover, paths involving the formation of charge-transfer intermediates may also become important at high exoergonicity, causing again an increase in the rate constant of the process with respect to the initial nonadiabatic plateau. In both cases, a step-wise behavior of the  $\log k_{12}$  vs.  $\Delta G$  plot is expected, although the observation of distinct plateaus is only possible if the new process becomes important when the old one is close to saturation and if the efficiencies of the two processes are sufficiently different. More generally, the presence of other reaction channels with increasing driving force will cause an increase in  $k_{12}$  which does not follow the predictions of eq 7 and 11.

As observed in the previous section, the involvement of more efficient channels with increasing driving force seems evident (Figure 3) for the electron-transfer reactions of europium ions. As discussed above, formation of f-d excited  $\text{Eu}^{2+}$  in  $\text{Eu}^{3+}$  reduction and of ligand-to-metal CT excited  $\text{Eu}^{3+}$  in  $\text{Eu}^{2+}$  oxidation would certainly offer less nonadiabatic (and thus more efficient) channels than those leading to the ground states. Such excited states, however, lie more than 3 eV above the ground state<sup>65</sup> and thus cannot be directly responsible for the efficient channels arising up at  $\sim -1$  eV for  $\text{Eu}^{2+}$  oxidation and  $\sim -0.5$  eV for  $\text{Eu}^{3+}$  reduction. By contrast, it seems reasonable that such channels correspond to reactions mediated by charge-transfer intermediates. For  $\text{Eu}^{3+}$  reduction, the availability at relatively low energy of an f-d excited state of the  $\text{Eu}^{2+}$  product (which corresponds to an electron in the outer d orbital) makes plausible the formation of a charge-transfer intermediate  $\text{Red}^{x+} \cdot \text{Eu}(\text{f}^6\text{d}^x)^{(3-x)+}$  involving partial donation ( $x < 1$ ) of a  $\pi^*$  electron of the Red species into the empty 5d orbital (complete charge transfer ( $x = 1$ ) would correspond to the generation of an f-d excited state of  $\text{Eu}^{2+}$ ). Deactivation of such an intermediate that can be considered as a nonspectroscopic CT state of the supermolecule consisting of the two redox partners in the encounter<sup>7</sup> can lead either back to the  $\text{Red} \cdot \text{Eu}^{3+}$  state (e.g., to the reactants) or to the more stable  $\text{Red}^+ \cdot \text{Eu}^{2+}$  ( $f^7$ ) state (e.g., to the redox products). Similarly, for  $\text{Eu}^{2+}$  oxidation the availability at relatively low energies of ligand-to-metal CT states of the  $\text{Eu}^{3+}$  product (which corresponds to a hole in a ligand orbital) makes plausible the formation of a charge-transfer intermediate  $\text{Ox}^{x-} \cdot \text{L}^{(1-x)-} \cdot \text{Eu}^{2+}$  involving partial ( $x < 1$ ) donation of a ligand electron into the empty  $t_{2g}$  metal orbital of the oxidant (complete transfer ( $x = 1$ ) would correspond to the formation of a ligand-to-metal CT excited state of  $\text{Eu}^{3+}$ ). Deactivation of this intermediate that can also be considered as another nonspectroscopic state of the system (see above) can lead either to the  $\text{Ox}^- \cdot \text{Eu}^{3+}$  products or back to the  $\text{Ox} \cdot \text{Eu}^{2+}$  reactants. It should be emphasized that both intermediates can be formed owing to the availability at relatively low energies of f-d and CT excited states in  $\text{Eu}^{2+}$  and  $\text{Eu}^{3+}$ , respectively. Thus such excited states are indirectly involved in these paths.

The direct or indirect involvement of excited states has an interesting consequence for the redox behavior of a redox couple. As long as the redox reactions involve the ground states, the reduction of the oxidized form (e.g.,  $\text{Eu}^{3+}$ ) and the oxidation of the reduced form (e.g.,  $\text{Eu}^{2+}$ ) are fully symmetric; i.e., the reduction and oxidation rate constants are equal if  $\Delta G$  is the same and the two partners are homogeneous. When excited states are involved, however, the symmetry is broken because in the outer-sphere mechanism the product of one reaction (e.g., the excited f-d  $\text{Eu}^{2+}$  in  $\text{Eu}^{3+}$  reduction) does not correspond to the reactant of the reverse reaction (e.g., ground-state  $\text{Eu}^{2+}$ ) and in the charge-transfer mechanism the two intermediates are different (see above). It is thus to be expected that the oxidation and reduction reactions exhibit different rates even when  $\Delta G$  is the same and the redox partners are homogeneous. Figure 3 suggests that reduction of  $\text{Eu}^{3+}$  and oxidation of  $\text{Eu}^{2+}$  at high exoergonicities may be examples of this behavior.

Finally, we note that the opening of more efficient reaction channels with increasing driving force evidenced by our analysis



is consistent with the notion that the electronically excited states which come into play at high exoergonicities are generally more available than the ground states for interactions with a redox partner.

### Conclusions

We have presented a new type of approach to the nonadiabaticity problem of outer-sphere electron-transfer reactions. The approach is based on the analysis of the behavior of the  $\log k_{12}$  vs.  $\Delta G$  plot for the reactions of the species under examination with a homogeneous family of redox partners. In favorable cases such an analysis allows disentangling of the effects of the intrinsic barrier (nuclear term) and nonadiabaticity (electronic term) on the rate constant. For  $\text{Ru}(\text{NH}_3)_6^{n+}$  and  $\text{Fe}^{n+}$  the plots indicate adiabatic or nearly adiabatic ( $\kappa \gtrsim 10^{-3}$ ) behavior in the  $\Delta G$  range 0 to  $-1.5$  eV, whereas for  $\text{Eu}^{2+}$  and  $\text{Eu}^{3+}$  the plots indicate that at moderately negative  $\Delta G$ , i.e., when the ground states of the ions are involved, electron transfer is strongly nonadiabatic. A theoretical estimate of the nonadiabaticity factor based on spectroscopic information shows that  $\kappa$  is  $\lesssim 10^{-5}$  for electron-transfer reactions between ground-state  $\text{Eu}^{2+}$  or  $\text{Eu}^{3+}$  and an adiabatic type partner and  $\lesssim 10^{-10}$  for the  $\text{Eu}^{2+}$ - $\text{Eu}^{3+}$  exchange. At large and negative  $\Delta G$  values more efficient but different channels become available for  $\text{Eu}^{2+}$  oxidation or  $\text{Eu}^{3+}$  reduction, as is generally expected because of the direct or indirect involvement of the excited states of the reaction products. The channels arising at  $\Delta G \approx -0.5$  eV for  $\text{Eu}^{3+}$  reduction and  $\approx -1$  eV for  $\text{Eu}^{2+}$  oxidation are proposed to involve different charge-transfer intermediates whose formation is made plausible by the presence at relatively low energies of f-d or CT excited states in  $\text{Eu}^{2+}$  and  $\text{Eu}^{3+}$ , respectively.

An important consequence of the nonadiabatic nature of the electron-transfer reactions of europium ions is that their rate constants cannot be used in or obtained from the original Marcus cross-reaction equation.<sup>2</sup> In fact, Sutin et al.<sup>15</sup> have already shown that when this is done, unreasonable results are obtained, like exchange rates for the  $\text{Eu}^{3+}$ - $\text{Eu}^{2+}$  couple varying by more than 4 orders of magnitude depending on the partner of the cross reaction whose rate constant was used in the calculation.

**Acknowledgment.** The authors wish to thank Dr. Norman Sutin for stimulating discussions.

### Appendix I

A homogeneous series of cross reactions (eq 1) has been defined as one in which  $k_e^0$ ,  $\Delta G^*(0)$ ,  $k_d$ ,  $k_{-d}$ , and  $k'_{-d}$  are constant. The requisite concerning the diffusion constants is quite obvious, and the appropriate corrections can be made, in case, as shown in Appendix II. As far as  $k_e^0$  and  $\Delta G^*(0)$  are concerned, it is convenient to split these parameters of the cross-reaction (eq 1) into intrinsic parameters of the two exchange processes (eq 8 and 9). This can be done by using the basic assumptions<sup>3</sup>

$$\Delta G^*(0) = \frac{\Delta G_{11}^* + \Delta G_{22}^*}{2} \quad (1a)$$

$$k_e^0 = \frac{kT}{h} \sqrt{\kappa_{11}\kappa_{22}} \quad (2a)$$

We can now define a homogeneous series of reactants as one in which  $\Delta G_{22}^*$  and  $\kappa_{22}$  are constant. If one species, e.g.,  $A_1$ , is reacted with a homogeneous series of reactants  $A_2$  of known  $\Delta G_{22}^*$  and  $\kappa_{22}$ , it is possible to obtain its unknown intrinsic parameters  $\Delta G_{11}^*$  and  $\kappa_{11}$  by using the approach outlined in Approach to the Nonadiabaticity Problem.

It may happen that in a series of reactants  $A_2$ , some are not homogeneous with the others. In these cases, it is possible to account for this nonhomogeneity provided that one of the intrinsic parameters ( $\kappa_{11}$  or  $\Delta G_{11}^*$ ) of the species under investigation is independently known. The procedure is as follows.

(1) Using the known  $\kappa_{22}$  and  $\Delta G_{22}^*$  values of the nonhomogeneous  $A_2$  species, the known intrinsic parameter ( $\kappa_{11}$  or  $\Delta G_{11}^*$ ) of the species under investigation, and eq 7, 11, 1a, and 2a, we performed trial calculations so as to determine the value of the unknown intrinsic parameter which best fits the experimental rate constant.

(2) The corrected ("homogenized") rate constant,  $k_{12}^{\text{corr}}$ , is obtained by recalculating  $k_{12}$  by means of eq 7, 11, 1a, and 2a, with the known and the obtained intrinsic parameters of  $A_1$ , and with the  $\kappa_{22}$  and  $\Delta G_{22}^*$  values appropriate to the homogeneous series of  $A_2$  reactants.

Among the  $A_2$  reactants of Table I,  $\text{Ru}(\text{NH}_3)_6^{n+}$ ,  $\text{Ru}(\text{NH}_3)_5\text{X}^{n+}$ , and  $\text{Ru}(\text{NH}_3)_4(\text{bpy})^{n+}$  are not homogeneous with the others (which all belong to the  $\text{M}(\text{LL})_3^{n+}$  family) because of higher intrinsic barriers. The correction for this nonhomogeneity has been done as described above, taking  $\kappa_{11} = 1$  and  $\kappa_{11} = 2.5 \times 10^{-3}$  for  $A_1 = \text{Ru}(\text{NH}_3)_6^{n+}$  and  $A_1 = \text{Fe}^{n+}$ ,<sup>13</sup> respectively. The  $\kappa_{22}$  and  $\Delta G_{22}^*$  values to be used in step 1 above were obtained from the  $k_{22}$  exchange rate constants  $4 \times 10^3 \text{ M}^{-1} \text{ s}^{-1}$  (0.1 M  $\text{NaClO}_4$ ) for  $\text{Ru}(\text{NH}_3)_6^{3+/2+}$ ,<sup>13</sup>  $4.7 \times 10^5 \text{ M}^{-1} \text{ s}^{-1}$  (1 M  $\text{CF}_3\text{SO}_3\text{H}$ ) for  $\text{Ru}(\text{NH}_3)_5\text{X}^{3+/2+}$ ,<sup>13</sup> and  $2.2 \times 10^6 \text{ M}^{-1} \text{ s}^{-1}$  (0.1 M  $\text{NaClO}_4$ ) for  $\text{Ru}(\text{NH}_3)_4(\text{bpy})^{3+/2+}$ ,<sup>5</sup> by using eq 3 and assuming an adiabatic behavior and appropriate  $K_0 = k_d/k_{-d}$  values. In step 2,  $\kappa_{22} = 1$  and  $\Delta G_{22}^* = 6 \text{ kcal/mol}$ <sup>16</sup> were used.

### Appendix II

If  $k_a$  and  $k_b$  are bimolecular rate constants of different electron-transfer processes having the same unimolecular electron-transfer rate constant  $k_e$ , the following relationship can be obtained by using eq 5 under the assumption (valid over the entire  $\Delta G$  range of this work) that  $k_{-e} \ll k'_{-d}$

$$\frac{1}{k_b} = \frac{1}{k_d^b} + \frac{k_d^a k_{-d}^b}{k_d^b k_{-d}^a} \left( \frac{1}{k_a} - \frac{1}{k_d^a} \right) \quad (3a)$$

Equation 3a can be used to homogenize bimolecular electron-transfer rate constants which differ in encounter distance ( $r$ ), charge product ( $z_{A_1}z_{A_2}$ ), and ionic strength ( $\mu$ ). This can be done by using the Debye<sup>69</sup> and Eigen<sup>70</sup> equations

$$k_d = \frac{8RT}{3000\eta} \frac{w_r/RT}{e^{w_r/RT} - 1} \quad (4a)$$

$$k_{-d} = \frac{2KT}{\pi r^3 \eta} \frac{w_r/RT}{1 - e^{-w_r/RT}} \quad (5a)$$

where  $w_r$  is given, according to the Debye-Hückel theory, by

$$w_r = \frac{z_{A_1}z_{A_2}Ne^2}{\epsilon r(1 + \beta r\sqrt{\mu})} \quad (6a)$$

$$\beta = \left( \frac{8\pi N^2 e^2}{1000\epsilon RT} \right)^{1/2}$$

In eq 4a, 5a, and 6a  $\eta$ ,  $\epsilon$ , and  $e$  are the viscosity, dielectric constant, and electron charge.

The homogenization performed by using this procedure is intended to compensate for gross differences in encounter distance, charge product, and ionic strength. The limited validity of eq 6a in accounting for the ionic strength is well-known and has also been recently discussed.<sup>5</sup>

The encounter distance  $r$  in the above equations is obtained as the sum of the individual radii of the reactants. The following values have been used for the radii:  $\text{M}(\text{LL})_3^{n+}$ , 7 Å;  $\text{Ru}(\text{NH}_3)_6^{n+}$ , 3.5 Å;  $\text{Ru}(\text{NH}_3)_5\text{X}^{n+}$ , 4 Å;  $\text{Ru}(\text{NH}_3)_4(\text{bpy})^{n+}$ , 4.5 Å;  $\text{Fe}^{n+}$ , 3.5 Å;  $\text{Eu}^{n+}$ , 4 Å.

(69) Debye, P. *Trans. Electrochem. Soc.* **1942**, 82, 265.

(70) Eigen, M. *Z. Phys. Chem. (Wiesbaden)* **1954**, 1, 176.